Australian Global Positioning Systems Society Inc.

Presented at SatNav 2003
The 6th International Symposium on
Satellite Navigation Technology Including
Mobile Positioning & Location Services

Melbourne, Australia
22–25 July 2003

Tropospheric delay corrections to differential InSAR results from GPS observations

Volker Janssen, Linlin Ge and Chris Rizos
Satellite Navigation and Positioning Group
School of Surveying and Spatial Information Systems
The University of New South Wales
Sydney NSW 2052, Australia
Tel: +61-2-9385 4208 Fax: +61-2-9313 7493 Email: v.janssen@student.unsw.edu.au

ABSTRACT

Differential Interferometric Synthetic Aperture Radar (DInSAR) techniques have been recognised as well-suited for ground deformation monitoring applications. However, the spatially and temporally variable delay of the radar signal propagating through the atmosphere represents a major limitation to accuracy. The dominant factor to be considered is the tropospheric heterogeneity, which can lead to misinterpretation of DInSAR results. In this paper a between-site and between-epoch double-differencing algorithm for the generation of tropospheric corrections to DInSAR results based on GPS observations is proposed. In order to correct the radar results on a pixel-by-pixel basis, the GPS-derived corrections have to be interpolated. Using GPS data from the Southern California Integrated GPS Network (SCIGN) it has been found that the inverse distance weighted and Kriging interpolation methods are more suitable than the spline method. Differential corrections as much as several centimetres may have to be applied in order to ensure sub-centimetre accuracy for the DInSAR result and it seems optimal to estimate the tropospheric delay from GPS data at 5-minute intervals. The algorithm and procedures described in this paper could easily be implemented in a continuous GPS data centre. The interpolated image of between-site, single-differenced tropospheric delay can be provided as a routine product to assist radar interferometry.

KEYWORDS: InSAR, GPS, tropospheric corrections, interpolation.

1. INTRODUCTION

Interferometric Synthetic Aperture Radar (InSAR) is a technique first suggested in the early 1970s (Graham, 1974). The technique produces an 'interferogram' from the phase difference between two SAR images acquired over the same geographical region. This interferogram contains three types of information: 1) *topographic pattern*, a contour-like pattern representing the topography of the area; 2) *geometric pattern*, a systematic striped pattern caused by differences between the two SAR sensor trajectories; and 3) *differential pattern*, fringes associated with any change of the range between the two SAR images, which can be due to ground displacement and/or change of atmospheric refraction. While the geometric pattern can be removed by modelling the geometry of the satellite orbits and ground targets, differential InSAR (DInSAR) has to be employed to remove the topographic pattern from the interferogram. In a typical European Remote Sensing Satellite (ERS) three-pass DInSAR procedure, two repeat-pass ERS-2 images will be processed to generate the interferogram (InSAR result 1), containing all the information mentioned earlier. A third ERS-1 image which forms a tandem pair with one of the two ERS-2 images is also introduced. The tandem pair with the ERS-2 satellite following the ERS-1 satellite one day later can be processed to generate the topographic pattern (InSAR result 2), because the deformation and growth of vegetation within one day can be neglected. By differencing the two InSAR results, the *residual* interferogram will contain only the differential pattern.

Due to its high spatial resolution, around-the-clock observation, ability of SAR to penetrate clouds, and cost effectiveness, DInSAR has definite advantages over many conventional deformation monitoring techniques. Many earthquake rupture zones and volcanoes have been studied using DInSAR (e.g., Massonnet *et al.*, 1993; Lu *et al.*, 1997). Studies, however, have shown that a change of atmospheric refraction (e.g. caused by a cold front moving across the region being imaged) can result in biases, which can lead to a misinterpretation of the DInSAR results (Zebker *et al.*, 1997; Hanssen *et al.*, 1999). Therefore, in order to reliably derive ground displacement from DInSAR results, it is crucial to correct for the atmospheric heterogeneity. This atmospheric heterogeneity can be partitioned into tropospheric and ionospheric components. In general, the troposphere can be divided into a wet layer (at about 0–10km above the surface) and a dry layer (at 10–50km). The ionosphere extends, in a number of distinct layers, from about 50km to 1000km above the Earth's surface. The SAR satellite orbit altitudes are typically in the range of 600–800km. The effect of the variations caused by the ionospheric layers lower than the SAR satellite altitude will be much smaller than that from the troposphere because the area penetrated by the radar is much smaller. Therefore, the ionospheric delay on the radar signal is usually considered to be uniform within one SAR image and can mostly cancel because the SAR images are acquired at the same time of the day, and hence the residual effect can be neglected. The tropospheric variations, however, can lead to misinterpretation of DInSAR results. While the dry portion of the tropospheric delay is well modelled, the wet portion is much more difficult to model because of the large variations of water vapour content with respect to time and space (e.g., Spilker, 1996).

Since 1997, researchers have been developing methodologies to correct InSAR results for these biases using measurements from other techniques, such as GPS (e.g., Bock and Williams, 1997; Ge *et al.*, 1997). In this paper, a between-site and between-epoch double-differencing algorithm for the generation of tropospheric corrections to DInSAR results based on GPS observations is proposed. The tropospheric parameters are interpolated in order to

enable the radar results to be corrected on a pixel-by-pixel basis. Experimental results generated from data collected in a continuous GPS network are presented.

2. MODELLING AND ESTIMATING THE TROPOSPHERIC DELAY WITH GPS

The troposphere can be defined as the electrically neutral (i.e. non-ionised) part of the atmosphere that stretches from the Earth's surface to a height of approximately 50km. The dominant impact of tropospheric path delay on radio signals occurs in the wet layer, typically below 10km (e.g., Spilker, 1996). The tropospheric delay is dependent on temperature, atmospheric pressure, water vapour content and the altitude of the GPS site. The tropospheric effect can be divided into two components, the dry and the wet component. The dry component accounts for about 90% of the refraction and can be accurately modelled using surface measurements of temperature and pressure. However, due to the high variation in the water vapour content, it is very difficult to model the remaining wet component.

Several models based on a 'standard atmosphere' have been developed to account for the tropospheric delay in the absence of accurate ground meteorological data (e.g., the Hopfield model, Saastamoinen model, Black model). As recommended by Mendes (1999), the Saastamoinen model has been used in this study. This model utilises the gas laws to deduce refractivity, and the tropospheric delay is therefore a function of zenith angle, pressure, temperature and the partial pressure of water vapour (Saastamoinen, 1973). For high-precision GPS surveys, an additional parameter can be introduced into the least squares reduction of the observations to estimate the *residual* tropospheric delay (after modelling). In this study, the Bernese GPS processing software was used to derive such tropospheric delay parameters for the individual stations of the network during parameter estimation. The user can specify the number of correction parameters to be estimated within the observation period.

3. DOUBLE-DIFFERENCING ALGORITHM FOR TROPOSPHERIC DELAY CORRECTIONS

Only the relative tropospheric delay (the tropospheric heterogeneity) between two SAR imaging points and between the two SAR image acquisitions will distort the deformation information derived by DInSAR, because it is the phase difference that is used and deformation is always referenced to an assumed stable point (site) in the image. Therefore, a between-site and between-epoch double-differencing algorithm can be used to derive the corrections to the DInSAR result from GPS observations. Assume that A is a stable site in the SAR image to be used as a reference point. B is another site in the same SAR image. If the tropospheric delay estimated from GPS for A and B at SAR imaging epoch j is denoted as D_A^j and D_B^j respectively, the between-site difference of the delays is:

$$D_{AB}^j = D_B^j - D_A^j \qquad (1)$$

Using site A as the reference, single between-site difference delays at other GPS sites can also be calculated, which are then interpolated (see next section) to generate a tropospheric delay image product similar to the radar SLC (single-look-complex) data. Assuming two sites A and B, and two epochs j (master SLC image) and k (slave image), two single-differences may be formed according to equation (1):

$$D_{AB}^{j} = D_{B}^{j} - D_{A}^{j}$$
$$D_{AB}^{k} = D_{B}^{k} - D_{A}^{k} \quad (2)$$

A double-difference is obtained by differencing these single-differences:

$$\begin{aligned} D_{AB}^{jk} &= D_{AB}^{k} - D_{AB}^{j} \\ &= (D_{B}^{k} - D_{A}^{k}) - (D_{B}^{j} - D_{A}^{j}) \\ &= (D_{B}^{k} - D_{B}^{j}) - (D_{A}^{k} - D_{A}^{j}) \end{aligned} \quad (3)$$

Equation (3) illustrates two possible approaches to double-differencing, either between-site (BS) differencing first and then between-epoch (BE) differencing (BSBE approach), or between-epoch differencing first and then between-site differencing (BEBS approach). The BSBE approach is preferred here because the BS difference can be interpolated to generate a single-difference correction product. This product will be associated with only the SLC image and hence can be used freely to form combinations for further BE differences as soon as InSAR pairs have been formed from SLC images.

4. INTERPOLATING TROPOSPHERIC DELAY CORRECTIONS

Continuous GPS networks may be as dense as one station every 25km at the national level, as is the case for the GEONET in Japan (GSI, 2003), or as dense as one station every few kilometres at the regional level, as is the case for the SCIGN in the USA (SCIGN, 2003). However, in order to correct the DInSAR result on a pixel-by-pixel basis (ERS SAR resolution ~25m), the GPS-derived tropospheric corrections have to be interpolated. In the following sections the utility of three commonly used interpolating methods will be discussed. Each interpolation technique makes assumptions about how to determine the estimated (interpolated) values. Depending on the phenomenon being modelled (i.e., here the differential tropospheric delay) and the distribution of sample points (in this case, GPS stations), one interpolator may produce better models of the actual surface (the tropospheric delay correction model) than others. Regardless of the interpolator, as a rule-of-thumb, the more input points and the more even their distribution, the more reliable the results.

4.1 Inverse Distance Weighted (IDW) Interpolation

The Inverse Distance Weighted interpolation (e.g., Lancaster and Salkauskas, 1986) explicitly assumes that things that are close to one another are more alike than those that are farther apart, i.e. they are spatially correlated. To predict a value for any unmeasured location, IDW uses the measured values surrounding the prediction location by weighting the points closer to the prediction location greater than those farther away, hence the name *inverse distance weighted*.

4.2 Spline Interpolation

This general-purpose interpolation method fits a minimum-curvature surface through the

input points (Schultz, 1973). Conceptually, this is like bending a sheet of rubber to pass through the points while minimising the total curvature of the surface. It fits a mathematical function (a minimum-curvature, two-dimensional, thin-plate spline) to a specified number of the nearest input points while passing through all input points. Therefore, the idea behind a spline fit is to approximate a function by a polynomial which is defined piecewise. For example, a cubic spline fit uses cubic polynomials which are defined over distinct, non-overlapping regions. The term *spline* means that the coefficients of the polynomial are chosen so that the following conditions are satisfied at the borders when two regions abut: (a) the values of the fit polynomials are the same, and (b) one (or more) of the derivatives match as well so that the slope (first derivative) is continuous. For cubic splines, it is possible to match the function values and first derivatives at both ends of the interval, resulting in a sufficiently smooth join for most purposes. This method is best for gradually varying surfaces. It is not appropriate when there are large changes within a short horizontal distance because it can overshoot estimated values. Hence, it would not be applicable to correct atmospheric interference induced by extreme weather conditions, which may be caused by a cold front moving across the area.

4.3 Kriging Interpolation

This interpolation method assumes that the distance or direction between sample points reflects a spatial correlation that can be used to explain variations in the surface. Kriging fits a mathematical function to a specified number of points, or all points within a specified radius, to determine the output value for each location. Kriging is a multistep process including exploratory statistical analysis of the data, variogram modelling, creating the surface, and (optionally) exploring a variance surface (Stein, 1999). Like IDW, Kriging weights the surrounding GPS-measured values to derive a prediction for a non-measured location. However, in IDW the weight depends solely on the distance between the measured points and the prediction location. Kriging also takes into account the overall spatial arrangement among the measured points by quantifying the spatial autocorrelation. Thus, the weight depends on a fitted model to the measured points, the distance to the prediction location, and the spatial relationships among the measured values around the prediction location. This function is most appropriate when there is a spatially correlated distance or directional bias in the data. It should be noted that Kriging uses the GPS-derived delay data twice: the first time to estimate the spatial autocorrelation of the data, and the second to make the predictions.

5. EXPERIMENTAL DATA ANALYSIS

Data from the Southern California Integrated GPS Network (SCIGN, 2003) were used to investigate the feasibility of the above methods to derive tropospheric delay corrections for DInSAR results from GPS observations. Of the 23 stations considered, 14 were treated as measured locations (reference stations) and 9 were used as prediction locations ('rover' stations) for which tropospheric delay corrections had to be interpolated and compared with their directly from GPS derived delays in a cross-validation procedure. A 2-hour session was observed on August 2, 2001 (DOY 214) and again on September 6, 2001 (DOY 249), simulating a typical ERS SAR satellite single repeat cycle of 35 days. Data were collected at a 30s sampling rate for a period of one hour before and after the flyover of the ERS-2 radar satellite. Figure 1 shows the location of the GPS sites within a typical ERS SAR image frame (the dashed lines) for this area. A close-up of the GPS sites, where the reference stations are

denoted by triangles, while the sites to be interpolated are indicated by circles, is also shown. For all sites, precise coordinates were obtained using the Scripps Coordinate Update Tool (SCOUT) provided by the Scripps Orbit and Permanent Array Center (SOPAC, 2003). This service computes the coordinates of a GPS receiver (whose data are submitted to the website) by using the three closest SCIGN reference sites and IGS final product precise GPS ephemerides. In this case, the coordinates were determined by taking the mean of six 24-hour solutions obtained in two blocks of three successive days (DOY 213-215 and 248-250). The average baseline lengths ranged from 2-7km. The repeatability of these six coordinate solutions was at the sub-centimetre level for all but one GPS site, indicating a solid, stable network. Site LBC1 showed relatively large coordinate variations indicating lower quality data or a likely displacement of 3.5cm and has therefore been left out of the subsequent interpolation.

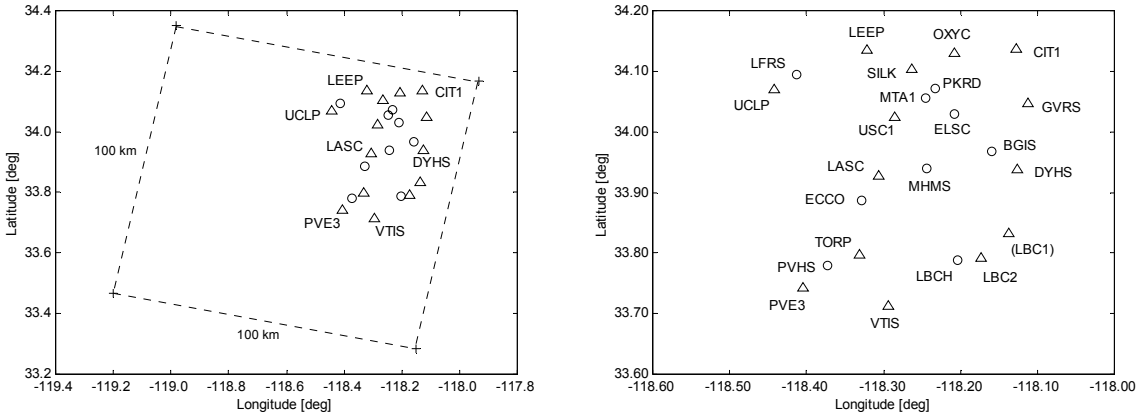

Figure 1. SCIGN stations within the ERS SAR image frame (left), and a close-up showing reference stations (triangles) and 'rover' stations (circles) (right)

5.1 GPS-derived Tropospheric Delay Corrections

The Bernese GPS processing software version 4.0 (Rothacher and Mervart, 1996) was used to process the network on both days, the coordinates of CIT1 being held fixed as the primary reference station. Baseline lengths vary from 7km to 49km, and the largest height difference is 270m. For each site, tropospheric delay corrections were determined every 20 minutes, resulting in six parameters per site throughout the 2-hour observation span. Single-differenced tropospheric corrections (equation 1) were then obtained by forming the differences relative to CIT1. These corrections range from –6.1cm to +2.2cm, and in some cases show variations of a few centimetres within the 2-hour observation span. DInSAR applications use two images of the same area in order to detect any ground deformation that might have occurred between the two satellite flyovers. To correct such a DInSAR image for the effect of the tropospheric delay, the relative *change* in the tropospheric conditions is of great importance. Hence double-differenced tropospheric corrections are obtained by forming the between-epoch difference of the single-differenced values derived in the previous step (equation 3). A comparison of the single- and double-differenced corrections revealed that almost all the double-differenced delay is smaller than the single-differenced delay (except for stations OXYC, MTA1 and PKRD). The double-differenced corrections range from –5.0cm to +3.3cm although the 23 stations spread over only a quarter of the SAR image frame (Figure 1). Therefore, it is crucial to apply such corrections in order for DInSAR to achieve sub-centimetre accuracy.

5.2 Interpolation of Tropospheric Delay Corrections

For each of the 9 'rover' sites (prediction locations) shown in Figure 1, the tropospheric delay corrections were interpolated using the three methods described in Section 4: IDW interpolation, spline interpolation and Kriging interpolation. Both the single-differenced tropospheric corrections relative to CIT1 for days 214 and 249, and the double-differenced tropospheric corrections between these two epochs were investigated by comparing the interpolated values to the 'true' values obtained directly using the Bernese software. This was done for each of the six 20-minute time intervals within the 2-hour observation span.

Figures 2-4 show the interpolation maps obtained for the different interpolation methods in the double-differenced case, which is most important and can be directly used for the correction of DInSAR results. The dots indicate the locations of the 22 GPS stations used in the analysis (refer to Figure 1 for their codes). The colour/grey step interval is 1mm. The main areas of tropospheric activity can be recognised in Figures 2-4, and the temporal and spatial variability of the tropospheric delay is clearly visible. The double-differenced interpolation values obtained with the different interpolation methods only differ by small amounts and are generally below or just above the cm-level. However, they do reach values of up to 3cm in some cases.

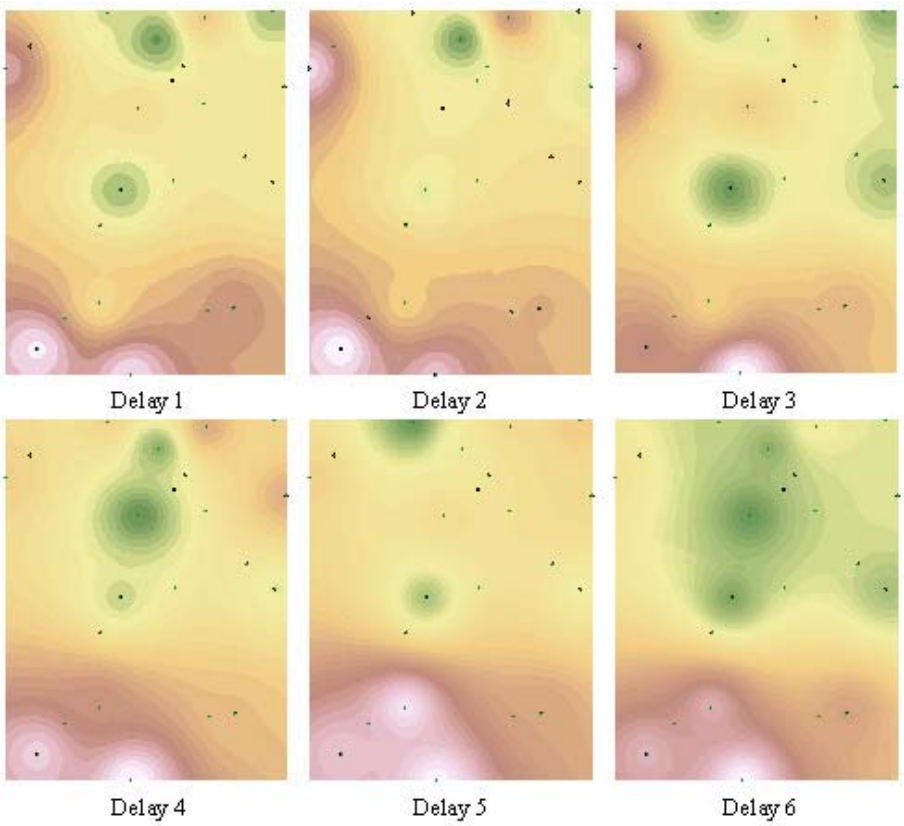

Figure 2. Interpolation maps for double-differenced tropospheric corrections (IDW)

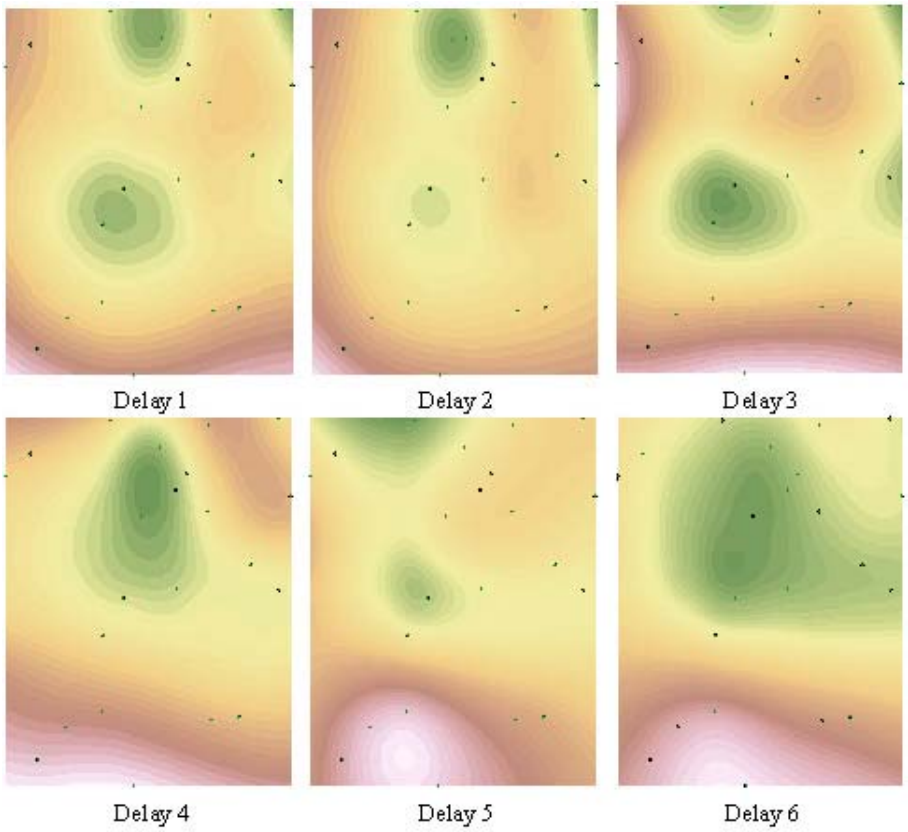

Figure 3. Interpolation maps for double-differenced tropospheric corrections (Spline)

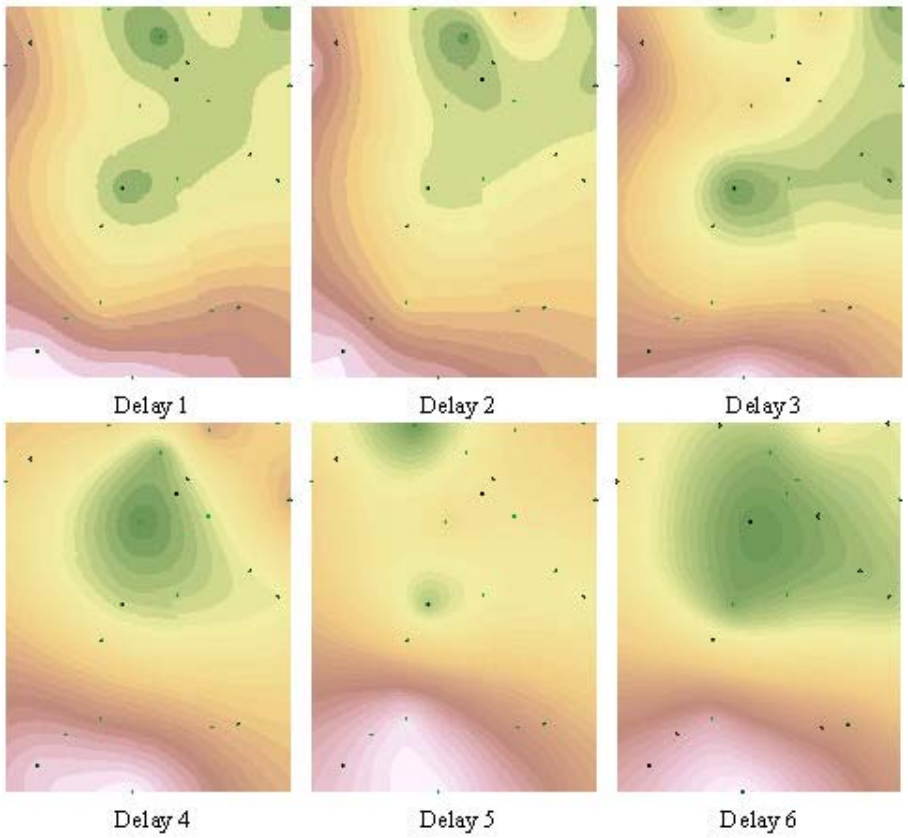

Figure 4. Interpolation maps for double-differenced tropospheric corrections (Kriging)

5.3 Which Interpolation Method Is The Most Suitable?

In order to determine which interpolation method gives the best results, the standard deviations of the results compared to the 'true' values obtained using the Bernese software were computed. The left graph of Figure 5 shows the standard deviations for the single-differenced case on days 214 (top plot) and 249 (middle plot), as well as for the double-differenced case (bottom plot). It is obvious that all three interpolation techniques deliver results with similar accuracy in this particular case, which is mostly at the sub-centimetre level. For the fourth time interval the accuracy is considerably lower compared to the rest of the observation span, almost reaching the 2cm level. This may have been caused by a short-term tropospheric event (e.g. weather front) on day 249, which again highlights the importance of applying the differential tropospheric delay corrections to InSAR results.

The tropospheric delay corrections are to be used to correct a set of InSAR images obtained from two SAR satellite flyovers. Hence it is important that the reference stations (GPS-measured locations) do not undergo any deformation between these two epochs. In practice, however, small movements may still occur, e.g. caused by tectonic events or nearby construction work. It is therefore useful to test the susceptibility of the interpolation techniques to outliers caused by small displacements in the reference stations or by reduced data quality. LBC1, a site that had earlier been identified as having a problem, was now included as a reference station in the interpolation process. The data were then processed again. The standard deviations of the resulting tropospheric corrections for the single-differenced case on days 214 (top plot) and 249 (middle plot), as well as for the double-differenced case (bottom plot), are shown in the right graph of Figure 5.

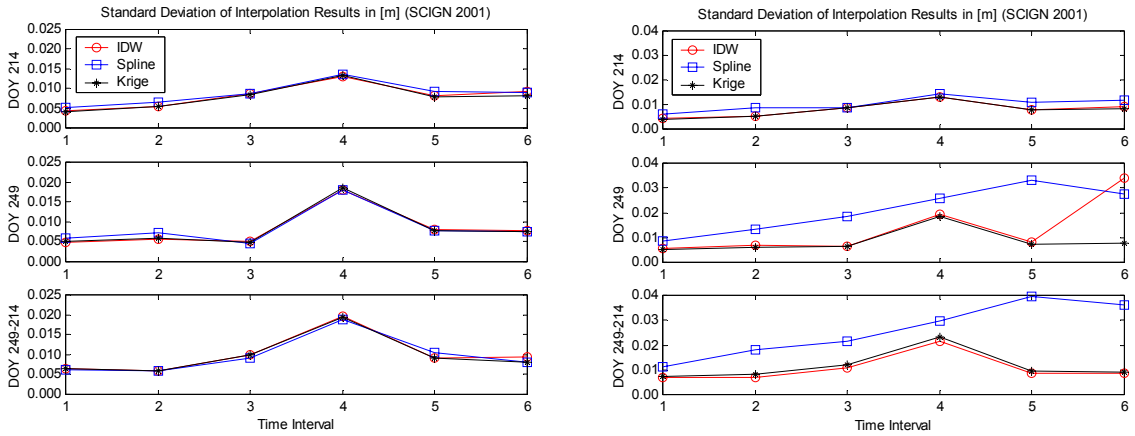

Figure 5. Standard deviation of the interpolation results obtained by different methods for a 'clean' reference network (left) and including an outlier (right)

It is obvious that the spline interpolation method has difficulties coping with such an 'outlier' in the reference station network. Standard deviations reach values of up to 4cm in the double-differenced case. The values for the IDW and Kriging interpolation techniques remain unchanged compared to the 'clean' reference network used in the previous case. Only the sixth time interval of the IDW interpolation on day 249 shows a change for the worse. However, this does not influence the double-differenced result (bottom-right graph of Figure 5), which indicates the robustness of the double-differencing algorithm proposed in this paper. It is therefore suggested that either the IDW or the Kriging interpolation method be used to determine tropospheric delay parameters from GPS observations. On the other hand, the two techniques can be used as a mutual check.

5.4 How Many Troposphere Parameters Should Be Determined?

The Bernese GPS processing software allows the user to specify the number of tropospheric delay parameters to be determined. Rothacher and Mervart (1996) recommend about 6-12 parameters for a 24-hour observation session. The estimation of one parameter for every 2-4 hours may be sufficient for geodetic control surveys where a set of coordinates is derived from a long observation session, taking into account all possible atmospheric effects. However, a special situation arises when one is dealing with GPS-derived tropospheric corrections for DInSAR. The SAR satellite will pass over the area of interest at a certain epoch and one is specifically interested in estimating the tropospheric delay as accurately as possible at this epoch within the observation span.

It is therefore necessary to determine how many parameters should be estimated in order to obtain an accurate representation of the tropospheric conditions at any point in time. A sub-network involving three GPS sites from the original network (Figure 1) was used. The baselines CIT1-UCLP and CIT1-VTIS are 30km and 49km in length with height differences of 104m and 156m respectively. The 2-hour session observed on September 6, 2001 (DOY 249) was processed several times incorporating a different number of estimable troposphere parameters. Tropospheric delay corrections were estimated for time intervals of 20, 10, 5 and 3 minutes in length, corresponding to 6, 12, 24 and 40 parameters per site respectively. Figure 6 shows the (single-differenced) tropospheric delay parameters for the sites UCLP (top) and VTIS (bottom), both relative to CIT1.

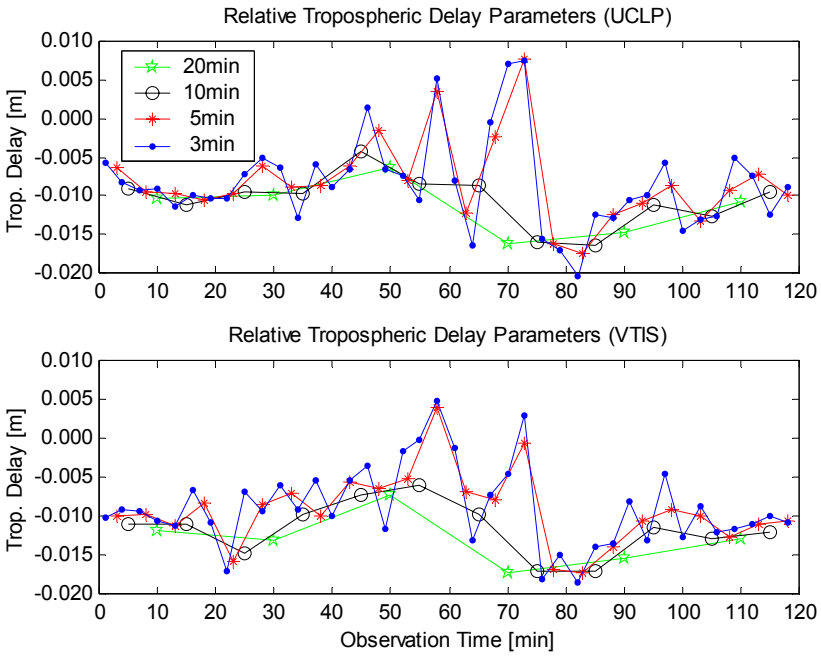

Figure 6. Relative tropospheric delay parameters for UCLP (top) and VTIS (bottom) over 2 hours

It is evident that both the 3min and 5min cases generate a rather detailed record of the variations in the troposphere. Short-term fluctuations are visible and values range from about +1cm to –2cm, even for the relatively small height differences of 100-150m between the stations. The 10min and 20min cases produce a smoothed representation of the tropospheric delay, which is obviously less likely to represent the correct conditions present at a specific

SAR time epoch. The resulting coordinates are practically the same for both the 3min and 5min tropospheric parameter estimation, with variations at the sub-mm level. If compared to the results obtained using 10min and 20min intervals, the coordinate differences are at the few-mm level. This corresponds to a difference of a few millimetres in the troposphere parameters between the 3min and 5min cases on the one hand and the 10min and 20min cases on the other (Figure 6). These results indicate that by estimating tropospheric delay parameters for 5-minute time intervals during a 2-hour observation session, the short-term variations of the troposphere can be reliably modelled. At the same time, the number of additional parameters to be estimated is still kept at a reasonable level.

6. CONCLUSIONS

Tropospheric heterogeneity (differential tropospheric delay) can lead to misinterpretation of DInSAR results. A between-site and between-epoch double-differencing algorithm has been proposed to derive tropospheric corrections to radar results from GPS measurements. These GPS observations can be made by either a network of continuous GPS (CGPS) stations or GPS campaigns synchronised to the radar satellite flyover. In order to correct the radar result on a pixel-by-pixel basis, the GPS-derived corrections have to be interpolated. Three interpolation methods (inverse distance weighted, spline, and Kriging) have been investigated. Using GPS data from the SCIGN network, it has been found that the inverse distance weighted and Kriging interpolation techniques are more suitable. Differential corrections as much as several centimetres may have to be applied in order to ensure sub-cm accuracy for the radar result. It seems optimal to estimate the tropospheric delay from GPS data at 5-minute intervals. The algorithm and procedures developed in this paper could be easily implemented in a CGPS network data centre. The interpolated image of between-site, single-differenced tropospheric delays can be generated as a routine product to assist radar interferometry, in a manner similar to the SLC radar images.

ACKNOWLEDGEMENTS: SCIGN and its sponsors, the W.M. Keck Foundation, NASA, NSF, USGS and SCEC, are acknowledged for providing the GPS data used in this study. Mr. Yufei Wang is thanked for his assistance during the interpolation process. This research is sponsored by grants from the ARC (Australian Research Council), ACARP (Australian Coal Association Research Program), and ESA (European Space Agency).

REFERENCES

Bock Y, Williams S (1997) Integrated Satellite Interferometry in Southern California, *Eos*, 78(29): 293

Ge L, Ishikawa Y, Fujiwara S, Miyazaki S, Qiao X, Li X, Yuan X, Chen W, Wang J (1997) The Integration of InSAR and CGPS: A Solution to Efficient Deformation Monitoring, *Proc. Int. Symp. on Current Crustal Movement & Hazard Reduction in East Asia and South-East Asia*, 4-7 November, Wuhan, P R. China, 145-155.

Graham, LC (1974) Synthetic Interferometer Radar for Topographic Mapping, *Proc. IEEE*, 62(6): 763-768

GSI (2003) http://mekira.gsi.go.jp/ENGLISH/index.html

Hanssen RF, Weckwerth TM, Zebker HA, Klees R (1999) High-Resolution Water Vapor Mapping from Interferometric Radar Measurements, *Science*, 283: 1295-1297

Lancaster P, Salkauskas K (1986) *Curve and Surface Fitting: An Introduction*, Academic Press, London-Orlando, 280pp

Lu Z, Fatland R, Wyss M, Li S, Eichelberger J, Dean K, Freymueller J (1997) Deformation of New

Trident Volcano Measured by ERS-1 SAR Interferometry, Katmai National Park, Alaska, *Geophysical Research Letters*, 24(6): 695-698

Massonnet D, Rossi M, Carmona C, Adragna F, Peltzer G, Feigl K, Rabaute T (1993) The Displacement Field of the Landers Earthquake Mapped by Radar Interferometry, *Nature*, 364: 138-142

Mendes VB (1999) Modeling the Neutral-Atmosphere Propagation Delay in Radiometric Space Techniques, *PhD Thesis*, Department of Geodesy & Geomatics Engineering Technical Report No. 199, University of New Brunswick, Fredericton, Canada, 353pp

Rothacher M, Mervart L (eds) (1996) *Bernese GPS Software Version 4.0*, Astronomical Institute, University of Berne, Switzerland, 418pp

Saastamoinen J (1973) Contributions to the Theory of Atmospheric Refraction, *Bulletin Géodésique*, 107: 13-34

Schultz MH (1973) *Spline Analysis*, Prentice-Hall, Englewood Cliffs, N.J., 156pp

SCIGN (2003): http://www.scign.org/

SOPAC (2003): http://sopac.ucsd.edu/cgi-bin/SCOUT.cgi

Spilker JJ (1996) Tropospheric Effects on GPS, in: Parkinson BW, Spilker JJ (eds), *Global Positioning System: Theory and Applications Volume 1*, Progress in Astronautics and Aeronautics, 163, American Institute of Aeronautics and Astronautics, Washington, 517-546

Stein ML (1999) *Interpolation of Spatial Data: Some Theory for Kriging*, Springer, New York, 247pp

Zebker HA, Rosen PA, Hensley S (1997) Atmospheric Effects in Interferometric Synthetic Aperture Radar Surface Deformation and Topographic Maps, *Journal of Geophysical Research*, 102(B4): 7547-7563